

Transport in ZnCoO thin films with stable bound magnetic polarons

Cite as: APL Mater. 2, 076101 (2014); <https://doi.org/10.1063/1.4886216>

Submitted: 13 April 2014 . Accepted: 15 June 2014 . Published Online: 01 July 2014

Tim Kaspar, Jan Fiedler, Ilona Skorupa, Danilo Bürger, Oliver G. Schmidt, and Heidemarie Schmidt



ARTICLES YOU MAY BE INTERESTED IN

Bound magnetic polarons and p - d exchange interaction in ferromagnetic insulating Cu-doped ZnO

Applied Physics Letters **98**, 162503 (2011); <https://doi.org/10.1063/1.3579544>

Calculation of Debye-Scherrer diffraction patterns from highly stressed polycrystalline materials

Journal of Applied Physics **119**, 215902 (2016); <https://doi.org/10.1063/1.4953028>

Theranostic mercury part 1: A new Hg/Au separation by a resin based method

AIP Conference Proceedings **1845**, 020023 (2017); <https://doi.org/10.1063/1.4983554>

additive manufacturing epitaxial crystal growth cerium oxide polishing powder silver nanoparticles sputtering targets

III-V semiconductors CVD precursors europium phosphors

AMERICAN ELEMENTS

THE ADVANCED MATERIALS MANUFACTURER®

gallium lump glassy carbon nanodispersions

InAs wafers laser crystals ultra high purity materials MOFs

organometallics quantum dots

rare earth metals photovoltaics refractory metals MOCVD

superconductors transparent ceramics ultra high purity silicon

deposition slugs OLED lighting spintronics solar energy

osmium nanoribbons thin films chalcogenides AuNPs

GDC li-ion battery electrolytes 99.999% ruthenium spheres

endothelial fullerenes copper nanoparticles diamond micropowder

CIGS MBE grade materials palladium catalysts flexible electronics

beta-barium borate borosilicate glass dysprosium pellets YBCO

pyrolytic graphite 3d graphene foam indium tin oxide mesoporous silica

raman substrates sapphire windows tungsten carbide InGaAs

barium fluoride carbon nanotubes lithium niobate scandium powder

Now Invent.™

The Next Generation of Material Science Catalogs

perovskite crystals yttrium iron garnet alternative energy h-BN

gold nanocubes graphene oxide macromolecules photonics

rhodium sponge fiber optics beamsplitters infrared dyes zeolites

fused quartz metallocenes platinum ink buckyballs Ti-6Al-4V

www.americanelements.com

American Elements opens up a world of possibilities so you can **Now Invent!**
Over 15,000 certified high purity laboratory chemicals, metals, & advanced materials and a state-of-the-art Research Center. Printable GHS-compliant Safety Data Sheets. Thousands of new products. And much more. All on a secure multi-language "Mobile Responsive" platform.



Transport in ZnCoO thin films with stable bound magnetic polarons

Tim Kaspar,¹ Jan Fiedler,¹ Ilona Skorupa,^{1,2} Danilo Bürger,²
 Oliver G. Schmidt,^{2,3} and Heidemarie Schmidt^{2,a}

¹*Institute of Ion-Beam Physics and Materials Research, Helmholtz-Zentrum Dresden-Rossendorf, Dresden 01328, Germany*

²*Faculty of Electrical Engineering and Information Technology, Chemnitz University of Technology, Chemnitz 09107, Germany*

³*Institute for Integrative Nanosciences, IFW Dresden, Dresden 01069, Germany*

(Received 13 April 2014; accepted 15 June 2014; published online 1 July 2014)

Diluted magnetic ZnCoO films with 5 at.% Co have been fabricated by pulsed laser deposition on c-plane sapphire substrates and Schottky and Ohmic contacts have been prepared in top-top configuration. The diode current is significantly reduced after the diode has been subjected to an external magnetic field. In the reverse bias range the corresponding positive magnetoresistance is persistent and amounts to more than 1800% (50 K), 240% (30 K), and 50% (5 K). This huge magnetoresistance can be attributed to the large internal magnetic field in depleted ZnCoO with ferromagnetic exchange between stable bound magnetic polarons. © 2014 Author(s). All article content, except where otherwise noted, is licensed under a Creative Commons Attribution 3.0 Unported License. [<http://dx.doi.org/10.1063/1.4886216>]

Magnetic semiconductors provide the capability of controlling the charge and spin of free charge carriers simultaneously. The clear understanding of magnetic, magnetotransport, and magneto-optical properties of magnetic semiconductors in an external magnetic and electric field is important for future semiconductor spintronics.¹⁻³ Generally, the wide bandgap semiconductor ZnO is *n*-type conducting due to intrinsic defects and exhibits a negligible weak negative magnetoresistance (MR) at 50 K. By alloying ZnO with isovalent 3*d* transition metal atoms, a large positive MR has been observed as long as the electron concentration *n* is below the critical electron concentration n_c ($n_c = 4 \times 10^{19} \text{ cm}^{-3}$). The MR dependence on *n* is one of the most characteristic features in magnetic ZnO films with the positive MR below ($n < n_c$) and the negative MR above ($n > n_c$).⁴ One major implication of our difficulty with the magnetization of the highly transparent and intrinsically *n*-type conducting magnetic ZnO is shallow and deep defects which have been studied, e.g., by deep level transient spectroscopy measurements.⁵ It has been concluded that impurities and other defects not only modify the electrical properties of magnetic ZnO, but may also mediate ferromagnetism.⁶ In this work we investigate hopping transport in the large internal magnetic field of depleted ZnCoO films with ferromagnetic exchange between stable bound magnetic polarons on insulating c-sapphire substrates. This work will help advancing the realization of stable bound magnetic polarons with ferromagnetic exchange in magnetic oxides.

As shown by deep level spectroscopy measurements most deep electron traps in magnetic ZnO follow the Meyer-Neldel rule and emit at the isokinetic temperature of 226 K with the same rate of 5996 s^{-1} .⁵ SQUID magnetization measurements⁷ excluded a dominating ferromagnetic coupling of Co ions in undepleted ZnCoO films. Note that the shallow Al donor⁸ may not serve as a center for bound magnetic polarons in ZnCoO. In a previous work we investigated the I-V characteristics of a Schottky diode in top-bottom configuration with a ca. 1 μm thick $\text{Zn}_{0.96}\text{Co}_{0.04}\text{O}$ film on an Al-doped ZnO bottom electrode⁹ where both Al impurities and oxygen vacancies caused the observed *n*-type conductivity in the $\text{Zn}_{0.96}\text{Co}_{0.04}\text{O}$. Furthermore, at zero bias the estimated

^aAuthor to whom correspondence should be addressed. Electronic mail: Heidemarie.Schmidt@etit.tu-chemnitz.de

depletion layer extended only over less than half of the $\text{Zn}_{0.96}\text{Co}_{0.04}\text{O}$ film.⁸ The diode current was decreased in a magnetic field and in the bias range from -0.5 V to $+0.5$ V, where leakage currents can be neglected and where the forward current is small. The observed reduction of the diode current was volatile in the whole bias range and amounted to 50% and 0.1% at 5 K and 50 K, respectively. We concluded that the field dependent current change is related with the positive magnetoresistance in ZnCoO due to the *s-d* exchange interaction induced splitting of the conduction band in an external magnetic field.⁴ In this work we prepared Schottky diodes with 74 nm thick $\text{Zn}_{0.95}\text{Co}_{0.05}\text{O}$ films on c-plane sapphire substrates by pulsed laser deposition (PLD) in top-top configuration without an Al-doped ZnO bottom electrode.¹⁰ The 74 nm thick $\text{Zn}_{0.95}\text{Co}_{0.05}\text{O}$ films have preferential c-axis orientation and are completely depleted at zero bias. We measured a huge positive magnetoresistance of more than 1800% (50 K), 240% (30 K), and 50% (5 K) and assigned it to the *s-d* exchange interaction induced splitting of the conduction band in the large internal magnetic field of stable bound magnetic polarons (BMP) with ferromagnetic exchange.

SQUID magnetization measurements show paramagnetic properties of undepleted ZnCoO films on sapphire substrates prepared under similar PLD growth conditions and without a Schottky contact. The rectangular Au/Ag_xO Schottky contact has an area of $A = 400 \times 50 \mu\text{m}^2$ (inset in Fig. 1). The current I between the Schottky contact (G in inset of Fig. 1) and Au/Ti Ohmic contact (S in inset of Fig. 1) was recorded under constant current conditions with a Lake Shore Model CPX-VF probe station. By applying a bias voltage V_{GS} to the Schottky diode the extension of the depletion region in the ZnCoO film below the Schottky contact is controlled. The rectifying behavior of the Schottky contact was confirmed by the asymmetric I - V characteristics in the temperature range from 5 K to 300 K (Fig. 1). In order to characterize the temperature dependent depletion, the real barrier height Φ_{Bn} , the ideal barrier height Φ_{B0} , and the ideality factor η of the Schottky diode have been modelled from I - V curves measured under dark conditions at different temperatures (Fig. 1). The charge carrier density n in the whole temperature range has been determined from Hall measurements on unstructured ZnCoO in van der Pauw geometry and the dominant transport mechanism has been deduced from the characteristic energy parameter E_{00} which in *n*-type semiconductors follows from

$$E_{00} = \frac{q\hbar}{2} \sqrt{\frac{n}{\epsilon_r \epsilon_0 m^*}}, \quad (1)$$

with m^* the effective electron mass, ϵ_r the relative permittivity, and n the charge carrier density. For the 74 nm thick ZnCoO film the condition $E_{00} \leq 0.5k_B T$ is fulfilled in the whole temperature range from 5 K to 300 K and we conclude that thermal emission (TE) over the Schottky barrier is the dominating transport mechanism. Therefore, we used the thermionic model to analyze the measured I - V curves (Fig. 1) and to determine the ideality factor η and the barrier height Φ_B from the measured current density J :

$$J = A^* T^2 \exp\left[\frac{e\Phi_B}{k_B T}\right] \cdot \left(\exp\left(\frac{e(V - IR_S)}{\eta k_B T}\right) - 1\right), \quad (2)$$

where J equals the normalized current I/A , A^* the Richardson constant, k_B the Boltzmann constant, T the temperature, and q the elementary charge. The results are presented in Fig. 2 and confirm an increasing ideality factor η and a decreasing barrier height with decreasing temperature (Fig. 2). This corresponds to degraded Schottky contact properties at low temperatures and is related with a decreasing charge carrier concentration n and an increasing series resistance R_S with decreasing temperature. Together with the barrier height Φ_B (Fig. 2) and the applied voltage V_{GS} the depletion layer width W is given by

$$W = \sqrt{\frac{2\epsilon_0 \epsilon_r (\Phi_B/e - V_{GS} - k_B T/e)}{qn}}, \quad (3)$$

where ϵ_0 is the dielectric constant. The relative permittivity ϵ_r of ZnCoO strongly increases with the Co concentration and amounts to $\epsilon_r \approx 25$ for 5 at.% Co in ZnCoO. At 300 K the charge carrier density is large and amounts to $6.7 \times 10^{16} \text{ cm}^{-3}$. Therefore, according to Eq. (3), at 300 K W amounts to only 118 nm. Obviously this is more than the thickness of the 74 nm thick ZnCoO film.

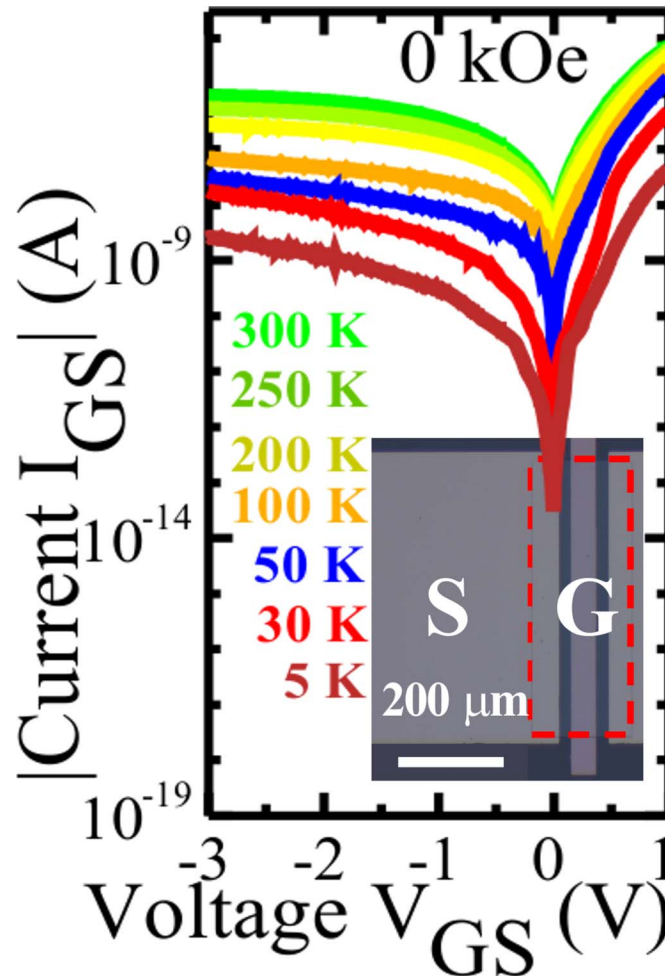


FIG. 1. Current-voltage characteristics of a Schottky diode in top-top contact configuration at 5 K, 30 K, 50 K, 100 K, 200 K, 250 K, and 300 K and at 0 kOe. (Inset) Partial photomicrograph of a MESFET structure with the 47 nm thick Au/Ag_xO Schottky (G) and the Ti/Au Ohmic (S) contact on a 74 nm thick ZnCoO film before deposition of the 14.5 nm thick Al₂O₃ passivation layer. The overlap area between the Au/Ag_xO Schottky contact (G) and the ZnCoO film amounts to $400 \times 50 \mu\text{m}^2$ and corresponds to the area A of the Schottky contact. The hidden edge of the ZnCoO film is emphasized by a red scattered line. For details on the preparation of the MESFET structure we refer to Ref. 10.

However, due to the tail of the thermal distribution of majority charge carriers in the depletion layer, above 0 K the width of the depletion layer in the abrupt approximation model with constant charge density is larger than the real depletion layer. As a consequence the completely depleted part of the ZnCoO film does not touch the underlying *c*-plane sapphire substrate at 300 K. The charge carrier density decreases with decreasing temperature to $1.8 \times 10^{16} \text{ cm}^{-3}$ and $3.4 \times 10^{15} \text{ cm}^{-3}$ at 50 K and 30 K, respectively. This correlates with an increasing depletion layer width of 680 nm at 50 K and of 1560 nm at 30 K. The main idea is to investigate completely depleted ZnCoO films with a very small free electron concentration ($n \ll n_c$) in order to realize ionized donors with a stable charge state in the center of BMPs in ZnCoO.

In the following the magnetotransport properties of the 74 nm thick ZnCoO films will be discussed in detail. After application of an external magnetic field we expect the magnetic moments of the BMP to align parallel. As long as the charge state of the ionized donors in the center of the BMP is not changed, the percolating state of the BMPs is retained also when the external magnetic field is removed. For EuO with $n < n_c$ it has already been shown that BMPs are formed in an external magnetic field¹¹ and strongly influence the magnetotransport properties of EuO. A first approach to determine internal magnetic fields related with percolating bound magnetic polarons has been

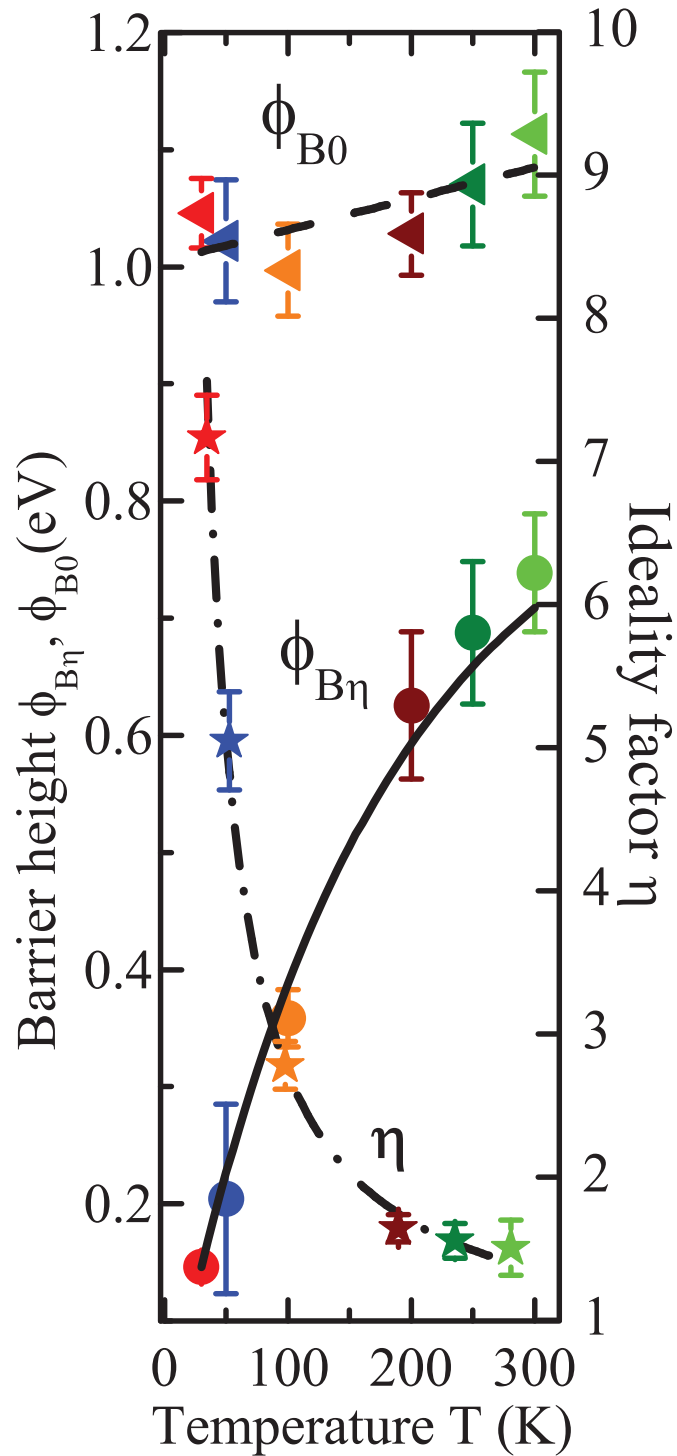


FIG. 2. Temperature dependent barrier height Φ_{B0} and $\Phi_{B\eta}$, and ideality factor η of the rectifying Au/Ag_xO gate contact (inset in Fig. 1). The barrier height $\Phi_{B\eta}$, and ideality factor η have been modelled from I-V characteristics at 30 K, 50 K, 100 K, 200 K, 250 K, and 300 K and at 0 kOe (Fig. 1) using Eq. (1). The ideal barrier height Φ_{B0} has been determined from Eq. (1) with an ideality factor $\eta = 1$.

reported in Ref. 12. Using time-resolved picosecond laser spectroscopy measurements a magnetic induction well in excess of 10 T has been estimated for percolating bound magnetic polarons in n -Cd_{0.9}Mn_{0.1}Se at 2 K.¹² From the I-V data measured on the diode at 50 K (Fig. 3(a)), at 30 K

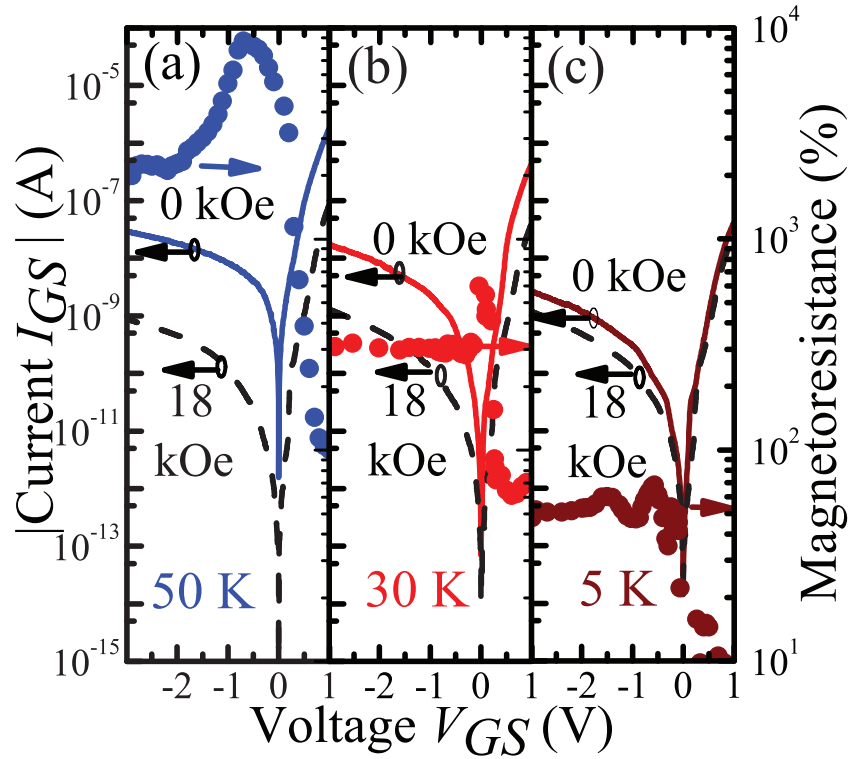


FIG. 3. Diode current on logarithmic scale at (a) 50 K, (b) 30 K, and (c) 5 K without applied external magnetic field (solid line) and with an applied magnetic field of 18 kOe (dashed line). The gate-source current I_{GS} is reduced by 1–2 orders of magnitude possibly due to the formation of percolating bound magnetic polarons in the depletion layer below the Au/Ag_xO gate contact in a magnetic field. The persistent, positive MR (dotted line) is constant in the bias range from -3 V to -1 V and has been calculated using Eq. (4) at 50 K (1800%), 30 K (240%), and 5 K (50%).

(Fig. 3(b)), and 5 K (Fig. 3(c)) without applied external magnetic field (solid line) and with an applied magnetic field of 18 kOe (dashed line) in constant-current conditions, we determined the magnetoresistance (MR) as follows:

$$MR = 100\% \cdot [V(H, I) - V(0, I)] / V(0, I). \quad (4)$$

A huge reduction of the diode current can be observed if the ZnCoO Schottky diode is exposed once to an external magnetic field. Even without magnetic field this current reduction is persistent below 50 K and reversible only if the ZnCoO diode is heated above 300 K. As for n -Cd_{0.9}Mn_{0.1}Se,¹² we attribute the corresponding positive magnetoresistance to the large effective internal magnetic field in ZnCoO with percolating bound magnetic polarons. We assume that stable percolating bound magnetic polarons are formed in depleted regions of ZnCoO after application of an external magnetic field and that the magnetic moments of bound magnetic polarons align parallel. The diode current with magnetic field is the same at 50 K, 30 K, and 5 K (Fig. 3). Only the diode current without magnetic field strongly increases with increasing temperature. Therefore, the calculated magnetoresistance (Eq. (4)) increases with increasing temperature. Mainly in the reverse bias range where the diode current is small the value of the magnetoresistance is huge and amounts to 1800%, 240%, and 50% at 50 K, 30 K, and 5 K, respectively. Oxygen vacancies in ZnO hold two electrons and are shallow donors, i.e., one of the electrons is loosely bound and can be easily depleted and one electron with s wavefunction is more tightly bound. The depleted electron leaves a hole with p wavefunction at the position of every oxygen vacancy. We expect that after application of an external magnetic field the magnetic moments of bound magnetic polarons are parallel aligned and percolate within the whole depletion layer.

The reduction of the diode current is persistent when the external magnetic field is zero again (not shown). After formation of stable bound magnetic polarons in the 74 nm thick Zn_{0.95}Co_{0.05}O

film in the reverse bias range, the persistent MR (1800% at 50 K) is more than 4 orders of magnitude larger (Fig. 3) than the volatile MR (0.1% at 50 K) in ca. 1 μm thick, only partially depleted ZnCoO films where no stable bound magnetic polarons are formed.⁹ From that we conclude that the positive MR in ZnCoO due to *s-d* exchange interaction is enhanced by a large internal magnetic field. In our previous work¹³ we investigated the MR of undepleted ZnCoO films without rectifying contacts where internal magnetic fields can be neglected and have modelled the MR of ZnCoO films by accounting for the quantum correction of *s-d* spin splitting on the disorder-modified electron-electron interaction (positive MR)¹⁴ and by accounting for the field-induced suppression of weak localization (negative MR).¹⁴

The extracted screening parameter for the Coulomb interaction F_σ (positive MR) increases with increasing temperature. And the dephasing length L_{Th} (negative MR) decreases with increasing temperature. We modelled the temperature dependent persistent and huge positive magnetoresistance of ZnCoO (Fig. 3) in the negative bias range under the assumption that the temperature dependent model parameters F_σ (positive MR) and L_{Th} (negative MR) from Ref. 13 in first approximation can also be used for nearly depleted ZnCoO. The effective magnetic ion concentration has been determined by modelling paramagnetic behavior of undepleted ZnCoO films without Schottky contact. The mobility of depleted ZnCoO has been obtained from modelling the transfer characteristics of MESFETs with a magnetic ZnCoO channel.¹³ We attribute the huge positive magnetoresistance (Fig. 3) to large internal magnetic fields and estimate a magnetic induction well in excess of 50 T. Up to our knowledge there are no other reports on persistent positive magnetoresistance in depleted diluted magnetic oxides above 50 K so far.

In summary pulsed laser deposition was used to grow 74 nm thick ZnCoO layers on c-plane sapphire substrates with a Co concentration of 5 at.%. The ZnCoO films have a charge carrier concentration below the metal-insulator transition of ZnO and reveal a large positive magnetoresistance at low temperatures due to *s-d* exchange interaction. Temperature and magnetic field dependent diode currents in ZnCoO have been measured between a rectifying Au/Ag_xO contact and a nonrectifying Au/Ti contact in top-top configuration. At low temperatures the ZnCoO films are completely depleted below the Au/Ag_xO Schottky contact and the diode current is persistently reduced after application of an external magnetic field due to the formation of bound magnetic polarons with ferromagnetic exchange.¹⁵ Charge carriers which are pulled through regions with percolating bound magnetic polarons are experiencing an increased path length due to Lorentz forces in the huge internal magnetic field of percolating BMP. Therefore, the charge carrier mobility is decreased in the depleted regions of the ZnCoO film. This effect is persistent at low temperatures and reversible only if the ZnCoO film is heated above 300 K. Therefore, magnetotransport in depleted ZnCoO is mainly determined by the internal magnetic field of the percolating bound polarons. We expect that models on scattering effects have to incorporate the effect of the intrinsic magnetic field in percolating bound magnetic polarons on the transport properties of charge carriers in the variable range hopping regime in diluted magnetic semiconductors. In the future we suggest to make the transport measurements on depleted and undepleted magnetic semiconductors a commonplace technique. For example, Hall bar structures from depleted and undepleted diluted magnetic semiconductors with and without rectifying contacts on the Hall bar, respectively, can be used to investigate hopping transport in the huge internal magnetic field of percolating BMPs. The observed magnetoresistance can be possibly used to switch the transport properties in circuitry with integrated magnetic semiconductors, e.g., optical isolators, magnetic sensors, and non-volatile memories, between two resistance states. We expect that such spintronics devices are another step towards low energy consuming information processing technologies.

The authors would like to acknowledge fruitful discussions with Professor M. Helm (HZDR) and financial support from the Initiative and Networking Fund of the Helmholtz Association (VH-VI-422) and from Deutsche Forschungsgemeinschaft (BU 2956/1-1, SCHM 1663/3-1, SCHM 1663/4-1).

¹N. A. Spaldin, *Magnetic Materials: Fundamentals and Applications* (Cambridge University Press, 2011), pp. 197–215.

²M. Johnson, *Spin Injection*, in *Spin Physics in Semiconductors* Vol. 157, edited by M. I. Dyakonov (Springer-Verlag, Berlin, 2008), pp. 279–308.

- ³Q. Y. Xu, L. Hartmann, S. Zhou, A. Mücklich, M. Helm, G. Biehne, H. Hochmuth, M. Lorenz, M. Grundmann, and H. Schmidt, *Phys. Rev. Lett.* **101**, 076601-1–076601-4 (2008).
- ⁴Q. Y. Xu, L. Hartmann, H. Schmidt *et al.*, *Phys. Rev. B* **73**, 205342-1–205342-5 (2006).
- ⁵H. Schmidt, M. Wiebe, B. Dittes, and M. Grundmann, *Appl. Phys. Lett.* **91**, 232110-1–232110-3 (2007).
- ⁶J. M. D. Coey, M. Venkatesan, and C. B. Fitzgerald, *Nat. Mater.* **4**, 173–179 (2005).
- ⁷M. Ivill, S. J. Pearton, S. Rawal, L. Leu, P. Sadik, R. Das, A. F. Hebard, M. Chisholm, J. D. Budai, and D. P. Norton, *New J. Phys.* **10**, 065002 (2008).
- ⁸J. H. Park, S. Lee, B.-S. Kim, W.-K. Kim, Y. C. Cho, M. W. Oh, C. R. Cho, and S.-Y. Jeong, *Appl. Phys. Lett.* **104**, 052412 (2014).
- ⁹Q. Y. Xu, S. Zhou, D. Bürger, H. Hochmuth, M. Lorenz, M. Grundmann, and H. Schmidt, *Jpn. J. Appl. Phys.* **49**, 043002-1–043002-4 (2010).
- ¹⁰T. Kaspar, J. Fiedler, I. Skorupa, D. Bürger, A. Mücklich, M. Fritzsche, O. G. Schmidt, and H. Schmidt, *IEEE Electron Dev. Lett.* **34**, 1271–1273 (2013).
- ¹¹J. Kübler, D. T. Vigen, *Phys. Rev. B* **11**, 4440–4449 (1975).
- ¹²J. H. Harris and A. V. Nurmikko, *Phys. Rev. Lett.* **51**, 1472–1475 (1983).
- ¹³Q. Y. Xu, L. Hartmann, H. Schmidt *et al.*, *Phys. Rev. B* **76**, 134417-1–134417-4 (2007).
- ¹⁴P. A. Lee and T. V. Ramakrishnan, *Rev. Mod. Phys.* **57**, 287 (1985).
- ¹⁵D. Emin, *Polarons* (Cambridge University Press, 2013), pp. 65–72.